polymer papers

Microphase separated structure and blood compatibility of segmented poly(urethaneureas) with different diamines in the hard segment

Atsushi Takahara, Jun-ichi Tashita, Tisato Kajiyama and Motowo Takayanagi
Department of Applied Chemistry, Faculty of Engineering, Kyushu University, Hakozaki, Higashi-ku, Fukuoka 812, Japan

and William J. MacKnight
Polymer Science and Engineering Department, University of Massachusetts, Amherst, Massachusetts 01003, USA
(Received 19 September 1983; revised 16 January 1984)

The properties, structures and blood compatibility by platelet adhesion and deformation of segmented poly(urethaneureas) (SPUU's) with various aliphatic diamine chain extenders were investigated. The SPUU's containing diamines with an odd number of methylene units showed a remarkable degree of phase mixing between the hard and soft segments. I.r. spectra of SPUU's indicated that the state of hydrogen bonding depended on the number of methylene units in the diamine. XPS measurements revealed that the surface concentration of soft segment was independent of diamine structure but the state of microphase separation strongly depended on the number of methylene units in the diamine. The SPUU's with an even number of methylene units in the diamines showed less platelet adhesion and deformation than those with an odd number of methylene units in the diamines.

(Keywords: blood compatability; microphase separation; hard segment; X-ray photoelectron spectroscopy (XPS); segmented poly(urethaneurea))

INTRODUCTION

Segmented poly(urethaneurea) (SPUU) is a multiblock copolymer consisting of an alternating sequence of hard and soft segments. Due to the incompatibility of hard and soft segments, phase separation occurs. The domain sizes of the hard segments estimated from small-angle X-ray scattering are 7 to 20 nm[1-4]. The hard segment domain acts as a physical crosslink due to its strong intermolecular hydrogen bonding between the urea groups.

In our previous paper, the properties and structures of SPUU's composed of 4,4'-diphenylmethane diisocyanate (MDI), ethylene diamine (EDA), and polyethers with various number average molecular weights ($\bar{M}_n$) were investigated[5-7]. The molar ratio of MDI, EDA and polyether diol for these SPUU's is 2:1:1. The glass transition temperatures of these SPUUs are shifted to higher temperatures with a decrease in $\bar{M}_n$ of the polyether. These results indicated that the microphase separation in SPUU is enhanced with an increase in $\bar{M}_n$ of the polyether. Wilkes and coworkers studied the morphology of SPUU prepared from 2,4-toluene diisocyanate (TDI), EDA and poly(tetramethylene glycol) (PTMG) by small-angle X-ray scattering (SAXS)[2]. The fact that the one dimensional correlation function of SPUU showed periodicity indicates microphase separation of the hard and soft segments of SPUU. Also, the SPUU containing PTMG with $\bar{M}_n$ of 2000 showed a higher value of the mean square fluctuation in electron density than that with $\bar{M}_n$ of 1000. This result indicates that microphase separation is enhanced with an increase in $\bar{M}_n$ of the PTMG.

Up to the present time, the studies on the structures and properties of SPUU have been limited mainly to SPUU varying $\bar{M}_n$ of the polyether or hard segment content. However, few attempts have been made to relate properties and various kinds of hard segment structures of SPUU. Bonart and coworkers carried out a structural study of SPUU with different diamine chain extenders by wide-angle X-ray diffraction[8]. They observed a difference in hydrogen bonding character between hard segments containing EDA and trimethylene diamine (TriMDA).

Recently, medical applications of SPUU's have been described as a result of their excellent mechanical strength and blood compatibility. The authors studied the blood compatibility of SPUU's based on MDI, EDA and various polyether diols which have different surface free energies and $\bar{M}_n$[4-7]. The most blood compatible surfaces are attained for SPUU's with $\bar{M}_n$ of 600–1000 for poly(ethylene glycol) (PEG), 1000 for poly(propylene glycol) (PPG), and 1900 for poly(tetramethylene glycol) (PTMG). These results revealed that the blood compatibility of SPUU was closely related to the degree of microphase separation and the surface free energy of the polyether[4-7].

In this study, the effects of diamine chain extender on properties, structures and blood compatibility of SPUU's

0032-3861/85/070978-09$03.00

were investigated. For this purpose, we synthesized SPUU's by using MDI, aliphatic diamines with different methylene chain lengths and polyether diols with $\bar{M}_n$ of 1000 for PEG and PPG, 1900 for PTMG at which SPUU's showed the best blood compatibility and mechanical strength in each series of polyether diols[4-7].

EXPERIMENTAL

Materials

Segmented poly(urethaneureas) (SPUU's) were synthesized by a two-stage modified solution polymerization method[9]. Polyether diols employed were poly(ethylene glycol) (PEG), poly(propylene glycol) (PPG) and poly(tetramethylene glycol) (PTMG), of which number average molecular weights ($\bar{M}_n$) were 1000, 1000 and 1900, respectively. These polyether diols were dehydrated under vacuum at 373 K for 3 h. The aliphatic diamines used in this experiment were hydrazine hydrate (HH), ethylene diamine (EDA), trimethylene diamine (1,3-propylene diamine) (TriMDA), tetramethylene diamine (TetMDA), pentamethylene diamine (PentMDA), hexamethylene diamine (HexMDA) and heptamethylene diamine (HeptMDA). Diisocyanate employed was 4,4'-diphenylmethane diisocyanate (MDI). MDI, TetMDA, PentMDA, HexMDA, HeptMDA and dimethyl sulphoxide (DMSO) were purified by vacuum distillation. EDA, TriMDA and methyl isobutyl ketone (MIBK) were purified by distillation at atmospheric pressure.

In the prepolymer reaction, 1 mol of the polyether diol was reacted with 2 moles of MDI at 388 K for 90 min in a 1:1 mixture of DMSO and MIBK. The prepolymer was cooled to room temperature and then reacted with 1 mol of aliphatic diamine for 60 min. The molar ratio of MDI, aliphatic diamine and polyether diol is 2:1:1. The entire synthesis was performed under a continuous purge of dried nitrogen. The SPUU was precipitated by pouring the polymerization solution into water. The precipitate was immersed in methanol for 15 h and washed with methanol. The SPUU's were dried *in vacuo* at 310 K for 10 h. The soft segment of SPUU consists of polyether diol and MDI. The hard segment is composed of alternating MDI and aliphatic diamine units.

Soft segment:

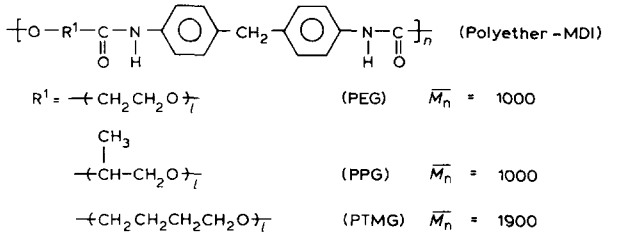

Hard segment:

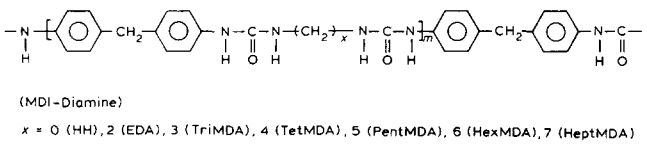

These SPUU specimens were designated 'X $\bar{M}_n$–Y' where X represents various types of polyether diol with number average molecular weight of $\bar{M}_n$ and Y represents diamine. For example, PTMG 1900–TriMDA denotes a SPUU containing the soft segment composed of PTMG with $\bar{M}_n$ of 1900 and MDI, and the hard segment composed of MDI and trimethylene diamine. Film specimens were cast on clean glass plate at 333 K from their dimethyl formamide (DMF) solutions. These film specimens were washed with ethanol and dried *in vacuo* at room temperature for more than a week. The complete removal of residual solvent in these SPUU's was confirmed from infra-red spectra.

Physical and structural characterization

Dynamic viscoelastic measurement. The temperature dependences of the dynamic mechanical viscoelastic responses were measured with a Rheovibron DDV II-C (Toyo Baldwin Co., Ltd.) at 11 Hz under a dried nitrogen purge.

Differential scanning calorimetry (d.s.c.). Thermal analyses were carried out with DSC UNIX (Rigaku Denki Co., Ltd.) in an atmosphere of dried nitrogen from 150 to 400 K. The sample weight was around 20.0 mg.

Infra-red measurements. Infra-red spectra were obtained from thin films of SPUU's using a Perkin–Elmer 567 Grating Infra-red Spectrometer.

X-ray photoelectron spectroscopy (XPS). The XPS spectra were obtained on a du Pont Model 650B photoelectron spectrometer employing a magnesium anode ($MgK\alpha = 1253.6$ eV) which was operated at 7 kV and 36 mA. The charging shift was referred to the C_{1s} line emitted from the saturated hydrocarbon.

Evaluation of blood compatibility of SPUU

Blood compatibility of SPUU was evaluated by the degree of interaction between blood platelets and the film surface of SPUU. Film specimens of SPUU were soaked in fresh human platelet rich plasma (PRP). These specimens were stored in PRP for 60 min at 310 K. Then, the films were rinsed with phosphate buffer solution (PBS: I = 0.2, pH = 7.4) under gentle agitation. The adhered platelets on the surface of SPUU were fixed with glutaraldehyde solution at 277 K for 15 h and dehydrated with acetone graded series. These films were coated with Au–Pd, and the morphology of the adhered platelets was observed with a scanning electron microscope S-430 (Hitachi Co., Ltd.).

RESULTS AND DISCUSSION

Physical and structural characterization

Differential scanning calorimetry. Figure 1 shows the d.s.c. thermograms of PPG 1000–Y with various aliphatic diamines. A sharp base line shift corresponding to the glass transition of the soft segment phase was observed in the temperature range between 240 to 270 K. The arrows in *Figure 1* indicate these glass transition temperatures, T_g's. PPG 1000–Y with diamines having odd numbers of methylene groups (abbreviated as odd diamines later) showed higher T_g's than those having even numbers of methylene groups (abbreviated as even diamines later). The PPG 1000–TriMDA showed the highest T_g and a broader glass transition zone in comparison with those of other SPUU's. Because all polymerizations of SPUU were carried out under the same conditions, it may be reasonable to consider that the sequential length of the hard and soft segments in SPUU's with odd diamines is

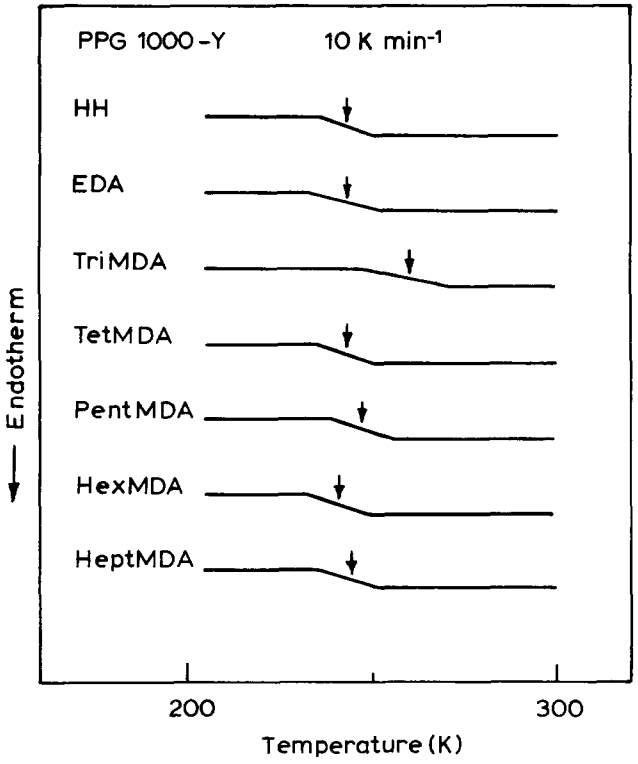

Figure 1 D.s.c. thermograms of PPG 1000–Y

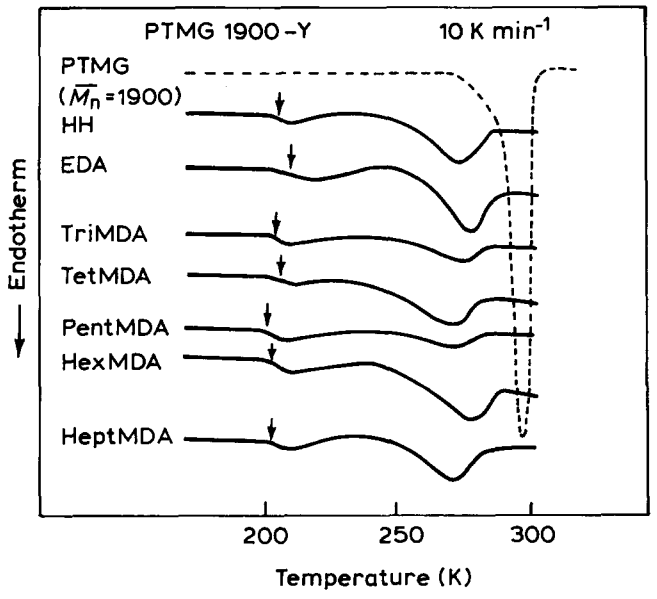

Figure 2 D.s.c. thermograms of PTMG 1900–Y and PTMG homopolymer ($\bar{M}_n$=1900)

almost identical to those with even diamines[10,11]. The phase mixing of soft and hard segments makes thermal molecular motion in soft segment phase restricted. Therefore, these shifts of T_g's to higher temperatures are attributed to the considerably strong interaction between hard and soft segments.

Figure 2 shows the d.s.c. thermograms for PTMG 1900–Y and PTMG homopolymer ($\bar{M}_n$=1900). Each specimen was heated above the melting temperature of PTMG and then quenched into liquid nitrogen. In the case of PTMG homopolymer, a sharp melting endotherm of PTMG crystals was observed at 290 K without any trace of glass transition behaviour, indicating the high crystallinity of PTMG homopolymer. PTMG 1900–Y exhibited a T_g at around 200 K, a broad crystallization exotherm over a temperature range of 230 to 240 K, and also a melting endotherm at around 270 K. The glass transition temperature of PTMG 1900–Y did not strongly depend on the odd and even diamine structure. Also, the location of the melting endotherm of PTMG is not strongly dependent on the number of methylene groups in the diamine. However, the areas of the melting peak of PTMG in PTMG 1900–TriMDA and PTMG 1900–PentMDA are smaller than those of the others. The relation between the crystallinity of PTMG in PTMG 1900–Y and the structure of the aliphatic diamine was used to evaluate the degree of microphase separation in these SPUU's, because the phase mixing of hard and soft segments reduces possibility of crystallization of PTMG chains. The relative crystallinity of PTMG in PTMG 1900–Y was determined from the area under the melting peak of PTMG in PTMG 1900–Y on the assumption that the degree of crystallinity of PTMG homopolymer ($\bar{M}_n$=1900) is 100%. *Figure 3* shows a plot of the relative degree of crystallinity of PTMG in PTMG 1900–Y against the number of methylene groups in the diamine of the hard segment. PTMG 1900–TriMDA and PTMG 1900–PentMDA show much lower degrees of crystallinity than the others. This may arise from the fact that the degree of microphase separation for PTMG 1900–TriMDA and PTMG 1900–PentMDA is less complete than in the others. The SPUU containing 1,2-propylenediamine as a chain extender did not show such a decrease in the crystallinity of PTMG. This fact reveals that the number of methylene groups along the main chain axis in the hard segment (odd and even) may affect the state of phase mixing. As reported elsewhere[6], the degree of phase separation between soft and hard segments proceeds with an increase in $\bar{M}_n$ of polyether in cases of PPG $\bar{M}_n$–EDA and PTMG $\bar{M}_n$–EDA. The degree of phase separation for PTMG 1900–EDA is more complete than that for PPG 1000–EDA on the basis of the magnitude of the T_g of the soft segment. Also, PTMG is more crystallizable than PPG. Then, in case of extensively phase separated SPUU such as PTMG 1900–Y, the relative crystallinity of the soft segment is a more sensitive criterion to evaluate the degree of microphase separation than T_g.

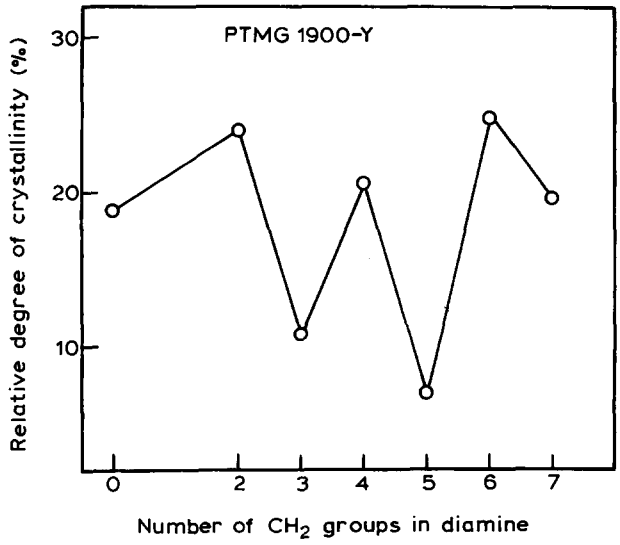

Figure 3 Variation of relative degree of crystallinity of PTMG in PTMG 1900–Y with number of methylene groups in diamine

Figure 4 represents the d.s.c. thermograms of PEG 1000–Y and PEG homopolymer ($\bar{M}_n = 1000$). PEG homopolymer did not show any base line shift corresponding to T_g due to high crystallinity. A large melting endotherm was observed at around 310 K. PEG 1000–Y showed the T_g of PEG around 230 K. PEG 1000–Y with odd diamines showed higher T_g's than those with even diamines. This indicates that PEG 1000–Y with odd diamines have greater phase mixing in comparison with PEG 1000–Y with even diamines. In the cases of PEG 1000–Y with even diamines, the small endotherm due to the melting of PEG crystals is observed at around 260 K. T_g behaviours and the appearance of a melting endotherm suggest that the interaction between hard and soft segments in PEG 1000–Y with even diamines is weaker than those with odd diamines. The d.s.c. data obtained for PEG 1000–Y, PPG 1000–Y and PTMG 1900–Y indicate that the hard segment structure affects the degree of microphase separation of SPUU.

Temperature dependences of dynamic viscoelasticity. Figure 5 represents the temperature dependences of the dynamic storage modulus, E', dynamic loss modulus, E'', (a) and mechanical loss tangent, tan δ (b) for PPG 1000–Y (Y = HH, EDA, TriMDA and HexMDA). PPG 1000–Y show a single major absorption as characterized by the peak curves in E'' and tan δ. We designated this relaxation as the α_a-process. The magnitude of the modulus decreases from 800 to 20 MPa over the α_a-relaxation range of 250 to 300 K. This α_a-absorption is associated with micro-Brownian segmental motion accompanying the T_g of the soft segment. PPG 1000–TetMDA shows similar dynamic viscoelastic behaviour to PPG 1000–HexMDA. The α_a-absorption appears at around 255 K for PPG 1000–Y with even diamines. In the cases of PPG 1000–PentMDA and PPG 1000–HeptMDA, the α_a-absorption peak is observed at about 5 K higher temperatures in comparison with those for PPG 1000–Y with even diamines. The α_a-absorption peak for PPG 1000–TriMDA appears at the abnormally high temperature of 271 K, which indicates extensive phase mixing of hard and soft segments in PPG 1000–TriMDA. These findings correspond to the d.s.c. results shown in *Figure 1*.

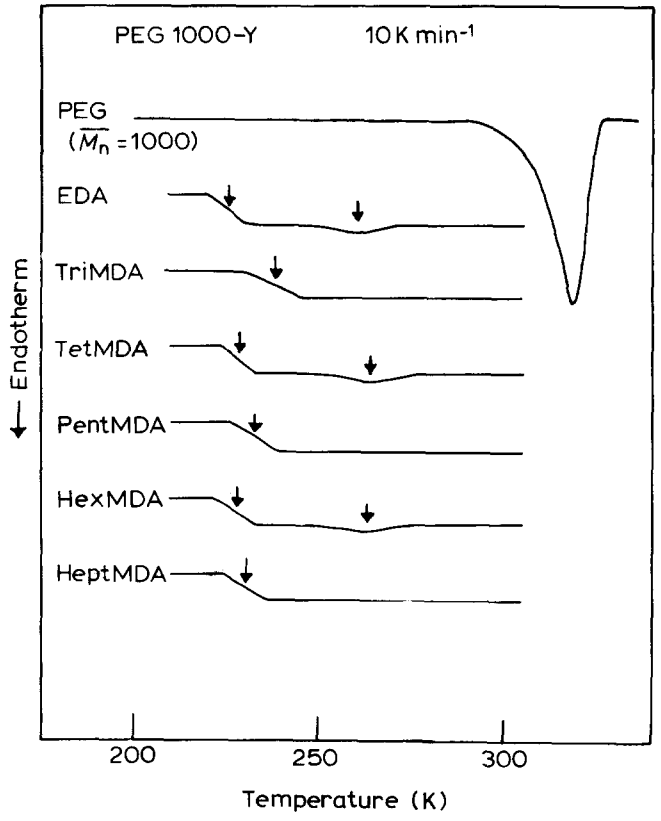

Figure 4 D.s.c. thermograms of PEG 1000–Y and PEG homopolymer ($\bar{M}_n = 1000$)

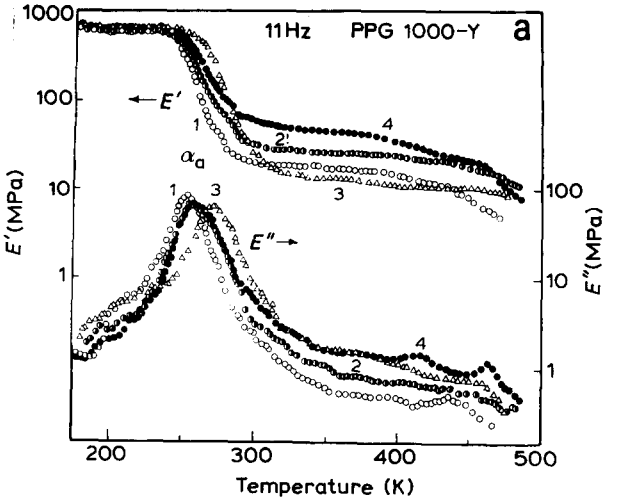

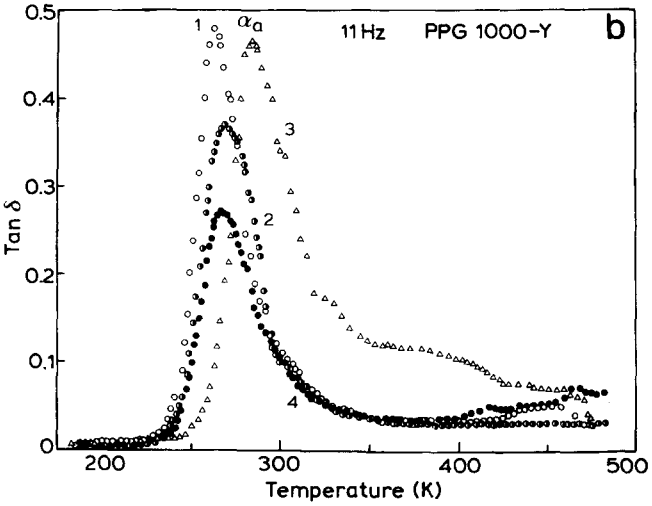

Figure 5 Temperature dependences of E', E'' (a) and tan δ (b) for PPG 1000–Y. ○, Y = HH; ◑, Y = EDA; △, Y = TriMDA; ●, Y = HexMDA

Figure 6 shows the temperature dependences of E', E'' (a) and tan δ (b) for PTMG 1900–Y (Y = HH, EDA and TriMDA). The dynamic viscoelastic behaviour of PTMG 1900–TetMDA and PTMG 1900–HexMDA were similar to that of PTMG 1900–EDA. The α_a- and γ-absorptions are located at 210 and 150 K, respectively. The γ-absorption was assigned to a local mode motion of methylene sequences in the soft (PTMG) segment. The α_a-absorption arises from micro-Brownian segmental motion of amorphous PTMG associated with the glass transition. The α_f-absorption was also observed at around 250 K as a shoulder of the α_a-absorption on the higher temperature side. This absorption is associated with a melting process in the crystalline phase of PTMG[12]. The dependence of the location of the α_a- and α_f-absorption

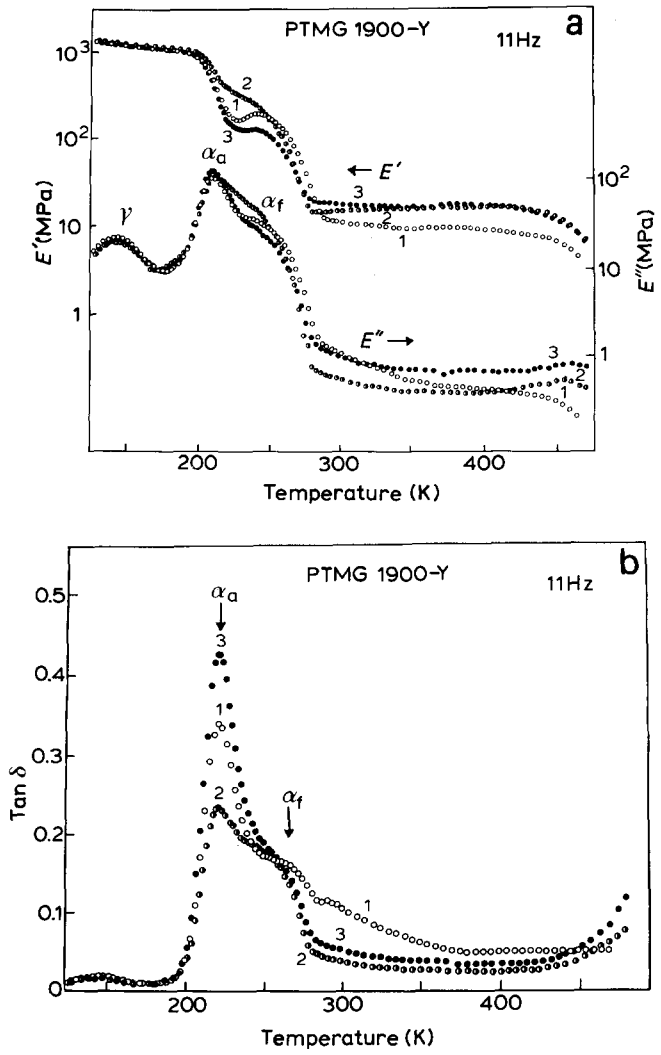

Figure 6 Temperature dependences of E', E'' (a) and tan δ (b) for PTMG 1900-Y. ○, Y=HH; ◑, Y=EDA; ●, Y=TriMDA

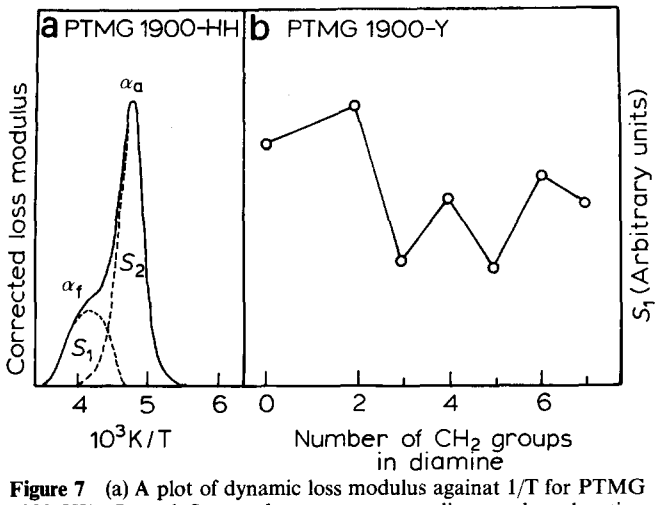

Figure 7 (a) A plot of dynamic loss modulus againat 1/T for PTMG 1900-HH. S_1 and S_2 are the area corresponding to the relaxation strength for α_f- and α_a relaxations. (b) Variation of α_f-relaxation strength of PTMG 1900-Y with number of methylene groups in diamine

peaks on the number of methylene groups in diamines is not clearly observed. In order to separate the E'' curve into the α_a- and the α_f-relaxation processes, the E'' curve over these relaxation temperature ranges was plotted against the reciprocal of the absolute temperature as shown on the left of *Figure 7*. Therefore, the relaxation strength of the α_f-relaxation process was evaluated from the area under resolved peaks of the $E''-1/T$ curve on the assumption of a single relaxation process. A base line was drawn from 170 to 290 K and overlapping peaks were resolved into two symmetrical peaks. S_1 and S_2 are the relative relaxation strengths for the α_f- and the α_a-relaxations, respectively. The right hand side of *Figure 7* represents the variation of relaxation strength for the α_f-relaxation process with the number of methylene groups in the diamine. The α_f-relaxation strengths for PTMG 1900–TriMDA and PTMG 1900–PentMDA (odd diamines) are smaller than those of others. This result corresponds to the d.s.c. result shown in *Figure 3*. Thus, the crystallization of PTMG in PTMG 1900–Y with odd diamines is impeded due to the considerable phase mixing of the hard and soft segments. This phase mixing may be closely related to the hydrogen bonding interaction between the ether oxygen in the soft segment and the urea or urethane group in the hard segment.

Infra-red spectra. Infra-red spectroscopy was used to investigate the structural difference in hard segments with various diamine structures. The i.r. spectra of PPG 1000–HH, PPG 1000–EDA and PPG 1000–TriMDA are shown in *Figure 8*. The assignments of several important bands are presented in *Table 1*. These assignments were based on the reports of Nakayama[13], Ishihara[14] and Stenzenberber *et al.*[15] The N–H absorption at 3320 cm^{-1}

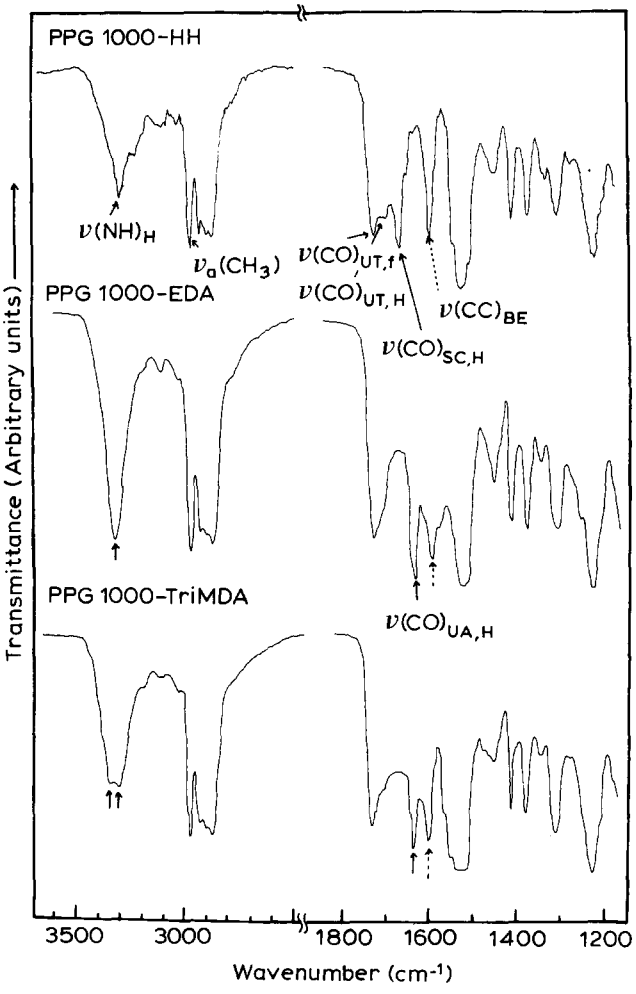

Figure 8 Infra-red survey spectra for PPG 1000–Y (Y = HH, EDA and TriMDA)

Table 1 Infra-red band assignments for SPUU's containing poly(propylene glycol) as a soft segment

Wavenumber (cm^{-1})[a]	Main assignment[b]
3500 vw	$\nu(NH)_{UA,UT}$ free
3320 s	$\nu(NH)_{UA,UT}$ H-bonded
3035 vw	$\nu(CH)_{BE}$
2970 s	$\nu_a(CH_3)_{PPG}$
2940 s	$\nu_a(CH_2)_{PPG}$
2880 vs	$\nu_s(CH_2)_{PPG}$
2800 m	$\nu_s(CH_2)_{PPG}$
1730 s	$\nu(CO)_{UT}$ free Amide I
1710 m	$\nu(CO)_{UT}$ H-bonded Amide I
1670 s	$\nu(CO)_{SC}$ H-bonded Amide I
1640 s	$\nu_{(CO)_{UA}}$ H-bonded Amide I
1600 s	$\nu(CC)_{BE}$
1581 w	$\nu(CC)_{BE}$
1547 vs	$\delta(NH)_{UA}+\nu(CN)_{UA}$ Amide II
1532 vs	$\delta(NH)_{UT}+\nu(CN)_{UT}$ Amide II
1520 m	$\nu(CC)_{BE}$
1450 m	$\delta(CH_2)_{PPG}$
1415 m	$\nu(CH_2)_{BE}$
1380 s	$\delta_s(CH_3)_{PPG}$
1310 m	$\beta(CH)_{BE}$
1230 s	$\delta(NH)_{UA,UT}+\nu(CN)_{UA,UT}$ Amide III

[a] Relative intensity: vs, very strong; s, strong; m, medium; w, weak; vw, very weak

[b] UA, urea group; UT, urethane group; PPG, poly(propylene glycol); BE, benzene ring; SC, aromatic semicarbazide in MDI–HH

associates with the stretching mode of hydrogen bonded N–H group. PPG 1000–Y with even diamines show a single maximum for the N–H absorption peak. However, PPG 1000–Y with odd diamines show a broadening of the N–H absorption peak, indicating that at least two states of hydrogen bonding exist in N–H of these SPUU's. The appearance of hydrogen bonded N–H absorption peak may be ascribed to the difference in the crystal structure of the hard segments of these SPUU's with odd and even diamines. The i.r. band at 1640 cm^{-1} associates with the hydrogen bonded urea carbonyl. In the case of PPG 1000–HH, the amide band I of the aromatic semicarbazide corresponding to the mode of 1640 cm^{-1} mentioned above is observed at 1670 cm^{-1}. The degree of hydrogen bonding in the hard segment is inversely related to the degree of aggregation of molecular chains in the hard segment. That is, the greater the degree of hydrogen bonding in the hard segment, the stronger the interaction between molecular chains in the hard segment and the better the phase separation between hard and soft segments.

Figure 9 shows the variation of the absorbance ratio of the hydrogen-bonded urea carbonyl (A(1640)) to the C=C stretching of the benzene ring (A(1600)) of PPG 1000–Y with the number of methylene groups in the diamine. The normalization by the C=C stretching of the benzene ring was carried out to correct for the film thickness. A base line was drawn from 1800 cm^{-1} to 970 cm^{-1}. $A(1640)/A(1600)$ denotes the relative hydrogen bonding concentration of the hard segment in these SPUU's. $A(1640)/A(1600)$ of PPG 1000–Y with odd diamines are smaller than those with even diamines. As the free urea carbonyl peak at 1695 cm^{-1} is not detected in these SPUU's, the urea carbonyls are almost completely hydrogen bonded. Since relative hydrogen bonding concentrations of urea carbonyls may closely relate to the state of the hydrogen bonding of the N–H, *Figure 9* indicates that molecular chains in the hard segment composed of even diamines and MDI form stronger interactions with each other and this strong aggregation induces an enhanced phase separation between the hard and soft segments.

Surface composition. Surface composition of SPUU was analysed by using X-ray photoelectron spectroscopy (XPS). *Figure 10* shows the XPS spectra for C_{1s}, N_{1s} and O_{1s} for the air facing surface (AFS) and the substrate facing surface (SFS) of PPG 1000–EDA solution cast on a clean glass plate. All spectra show three carbon, one nitrogen and one oxygen peaks. The C_{1s} peak corresponding to the aliphatic and aromatic carbons was observed at 285.0 eV. The C_{1s} peak for ethereal carbon is located at 286.3 eV. The C_{1s} peak corresponding to the carbonyl carbon of the urethane and urea groups was observed as a small shoulder at 288.8 eV. The N_{1s} peak is located at 400.3 eV, corresponding to the nitrogen of the urea and urethane groups. The O_{1s} peak appears at 532.9 eV, corresponding to the oxygen of the polyether and urethane and urea carbonyl. The intensity of the C_{1s} peak from the ethereal carbon is larger in the AFS than that in the SFS. Also, the ratio of the intensity of the O_{1s} to N_{1s} peaks on the AFS is larger than that on the SFS. Elemental analysis of PPG $\bar{M}_n$–EDA revealed that the number ratio of oxygen atoms to nitrogen atoms increased with an increase in $\bar{M}_n$ of the polyether, as expected from calculations of the total number of oxygen and nitrogen atoms. *Figure 10* indicates that the PPG component is abundant on the AFS due to the lower surface free energy of PPG than that of the hard segment.

The number ratio of oxygen atoms to nitrogen atoms, O/N was adopted for a measure of relative soft segment concentration. The value of O/N was evaluated by the method reported elsewhere[7,16]. *Figure 11* shows a plot of O/N against the number of methylene groups in the diamine for PPG 1000–Y. The broken line indicates the

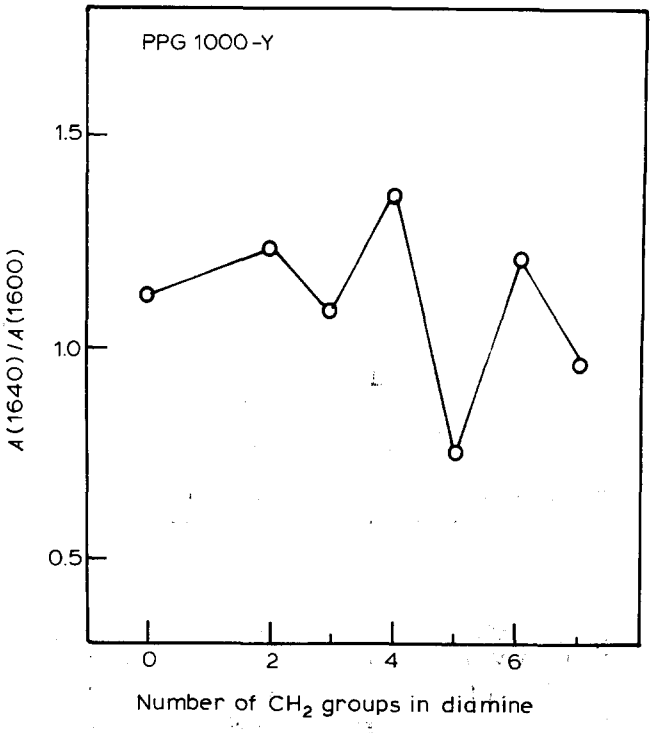

Figure 9 Variation of $A(1640)/A(1600)$ of PPG 1000–Y with number of methylene groups in diamine

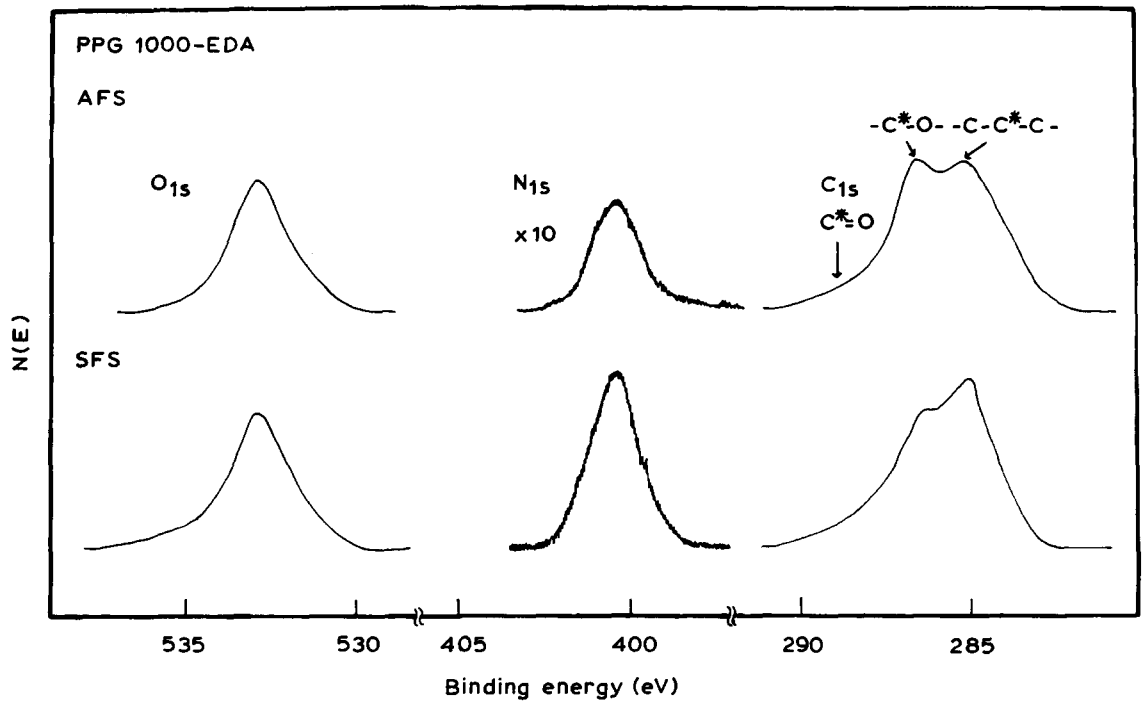

Figure 10 X-ray photoelectron spectra for PPG 1000-EDA. AFS and SFS are air and substrate facing surfaces, respectively

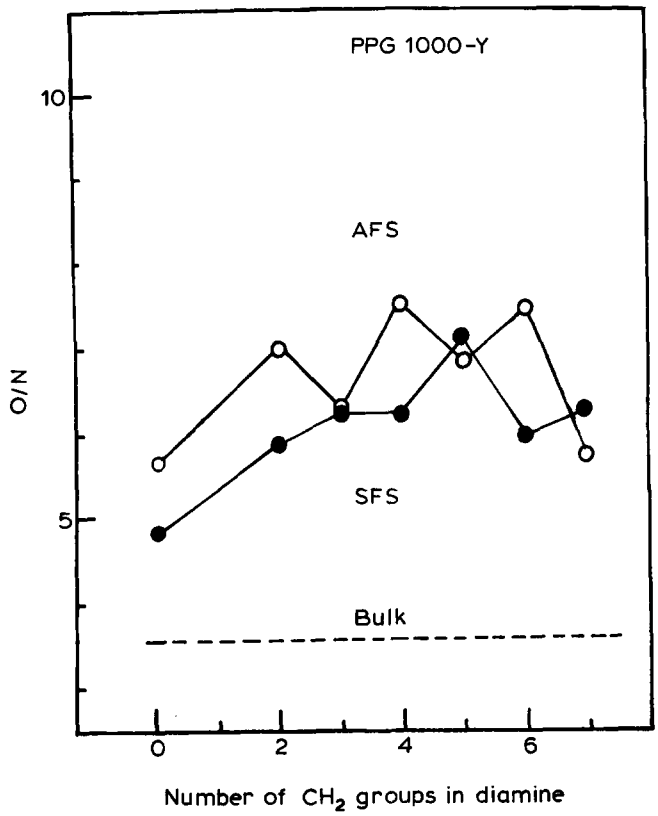

Figure 11 Variation of number ratio of oxygen atoms to nitrogen atoms, O/N of PPG 1000-Y with number of methylene groups in diamine

magnitude of O/N from elemental analysis. In the case of PPG 1000-Y with even diamines, the value of O/N on the AFS is larger than that on the SFS. In other words, the concentration of soft segment on the AFS is greater than that on the SFS. This anisotropic distribution of hard and soft segments on the AFS and SFS is due to the difference in surface free energy of each segment[7]. In the cases of PPG 1000-Y with odd diamines, the anisotropic distribution of hard and soft segments is not remarkable on the AFS and SFS in comparison with the case for the even diamines. *Figure 11* apparently tells us that the phase mixing of the hard and soft segments is more prominent in the case of SPUU with odd diamines.

Blood compatibility

The degree of interaction between blood platelets and the polymer surface is closely related to the thrombogenicity of the polymers. The blood compatibility of SPUU was evaluated from counting the number of adhered deformed platelets on the film surface of SPUU. *Figure 12* shows scanning electron photomicrographs of the typical morphology of the adhered platelets on the substratum. The morphology of adhered platelets was classified into three types based on the degree of deformation[4-7,18]:

(I) attachment of platelets at a point of contact with substratum;

(II) centrifugal growth of filopodia;

(III) cytoplasimic webbing and flattening of the central mass.

Since the deformation of adhered platelets proceeds in order of I, II and III with time, these morphological observations may be applied as a measure of blood compatibility. In the case of type I, the interaction between substrate and platelets is weak and adhered platelets can be easily removed during rinsing with phosphate buffer solution.

Since the platelets of types II and III strongly adhere to the substrate, the number of adhered platelets of these types (number of deformed platelets) would be an index of thrombogenicity.

Figure 13 represents the variation of the number of adhered (total) and deformed (II+III) platelets on the AFS of PPG 1000-Y with the number of methylene groups in the diamine. PPG 1000-Y with odd diamines

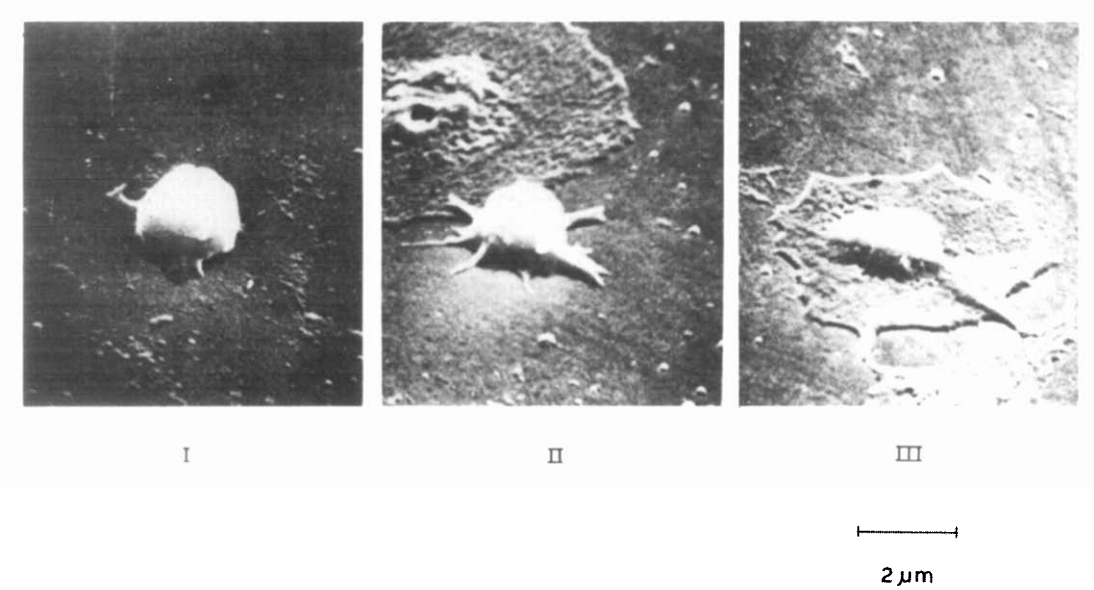

Figure 12 Scanning electron photomicrographs of three types of adhered platelets on surface of substratum

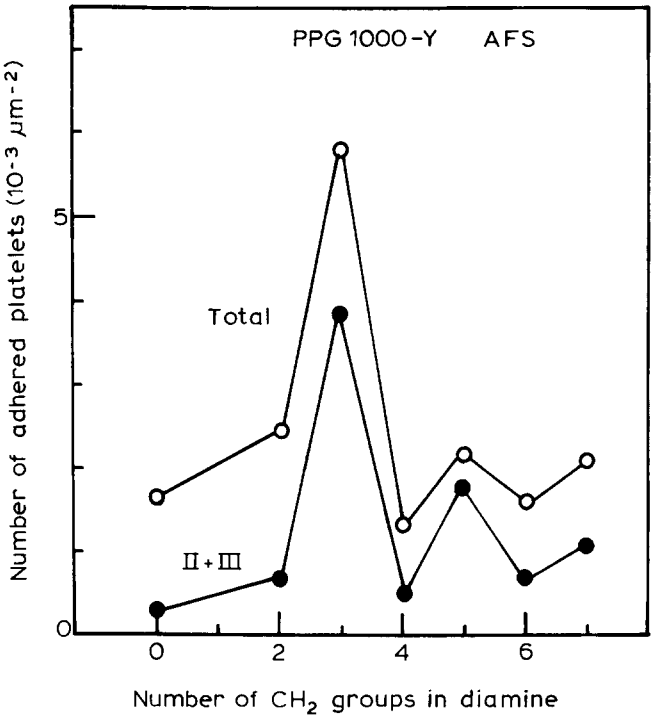

Figure 13 Variation of number of adhered (Total) and deformed (II+III) platelets on AFS of PPG 1000–Y with number of methylene groups in diamine

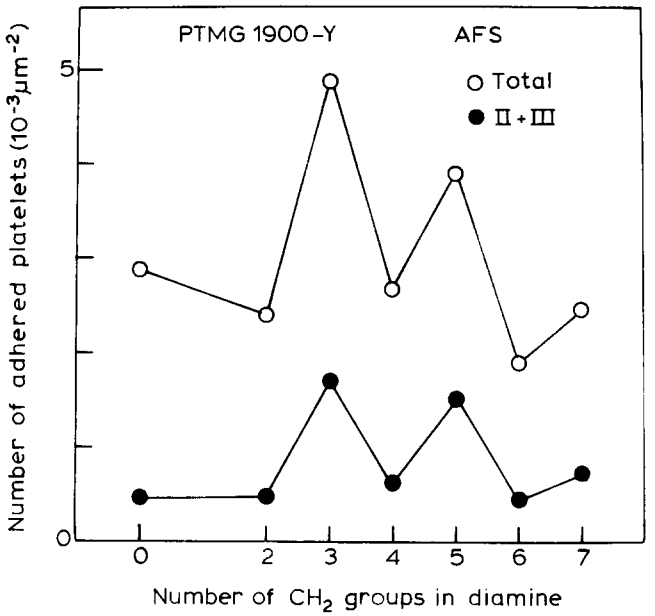

Figure 14 Variation of number of adhered (Total) and deformed (II+III) platelets on AFS of PTMG 1900–Y with number of methylene groups in diamine

are less blood compatible than those with even diamines. The number of adhered and deformed platelets on PPG 1000–TriMDA is extensive. The inferior blood compatibility of PPG 1000–TriMDA may be attributed to an increase in phase mixing of hard and soft segments as shown in *Figures 1*, *5* and *9*. It seems apparent from comparison of *Figures 1* and *13* that the order of thrombogenicity may correspond to the order of T_g.

Figure 14 shows the variation of the number of adhered (total) and deformed (II+III) platelets on the AFS of PTMG 1900–Y with the number of methylene groups in the diamine. As observed in PPG 1000–Y, PTMG 1900–Y with odd diamines are also less blood compatible than those with even diamines. In this case, it seems apparent from comparison of *Figures 3* and *14* that the order of the number of deformed platelets corresponds to the reverse order of relative crystallinity of PTMG in PTMG 1900–Y. That is, the blood compatibility of PTMG 1900–Y is improved with an increase in crystallinity of PTMG. Similar trends were observed for PEG 1000–Y. Since the distribution and sequential length of the hard and soft segments in SPUU are comparable under the same polymerization conditions, the domain size of the hard segments of these SPUU's slightly increased with an increase in diamine length. Since there is no direct relationship between blood compatibility and domain size for PTMG 1900–Y, the domain size of microphase separated structure is not an important factor for blood compatibility of PTMG 1900–Y.

Figure 15 shows a plot of the number of deformed platelets on the AFS of PPG $\bar{M}_n$–Y against the surface concentration of the soft segment, O/N. Open circles

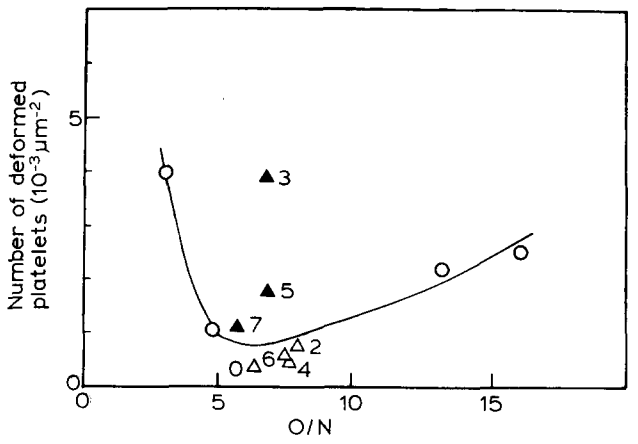

Figure 15 Relationships between number of deformed platelets and O/N on AFS of PPG $\bar{M}_n$–Y. ○, PPG $\bar{M}_n$–EDA; △, PPG 1000–Y (Y=HH, EDA, TetMDA and HexMDA); ▲, PEG 1000–Y (Y=-TriMDA, PentMDA and HeptMDA). Numbers beside each symbol denote number of methylene groups in diamine

represent PPG $\bar{M}_n$–EDA with various $\bar{M}_n$ of PPG. Open and closed triangles represent PPG 1000–Y with even and odd diamines, respectively. In the case of PPG $\bar{M}_n$–EDA, O/N increases with an increase in $\bar{M}_n$ of PPG and the number of deformed platelets shows a minimum at O/N = 6.5 corresponding to $\bar{M}_n = 1000$. The existence of the minimum number of deformed platelets at O/N = 6.5 indicates that there is an optimum condition of hydrophobic and hydrophilic balance for excellent blood compatibility[7]. In the case of PPG 1000–Y, the magnitude of O/N does not depend on the diamine structure but the number of deformed platelets on PPG 1000–Y with odd diamines (▲) is larger than those with even diamines (△) as shown in *Figure 15*. Since the chemical structure of the soft segment is the same in case of PPG 1000–Y, the surface concentration of soft segment is independent of diamine structure. However, the degree of microphase separation of the hard and soft segments is strongly affected by diamine structure as shown by d.s.c., dynamic mechanical, infra-red spectroscopic and XPS experiments. Though the mechanism of thrombus formation at the interface between SPUU and blood is not clearly understood at present, the apparent phase separation of the hard and soft segments produces excellent blood compatibility.

CONCLUSIONS

D.s.c., dynamic mechanical, infra-red spectroscopic and XPS measurements were carried out in order to characterize the aggregation structure of SPUU's with various aliphatic diamine chain extenders. Also, the blood compatibility of these SPUU's were investigated in order to characterize their biomedical performance.

The SPUU's with odd diamines showed higher T_g's or α_a-relaxation temperatures than those with even diamines. This result indicates the thermal molecular motion of the soft segment is effectively restricted by the phase mixing of the hard and soft segments. XPS measurements revealed that the surface anisotropy of composition of hard and soft segments depended on diamine structure, and anisotropy of composition on AFS and SFS became less owing to high phase mixing of hard and soft segments.

The blood compatibility of SPUU was evaluated by the degree of interaction between blood platelets and the surface of SPUU. The number of adhered and deformed platelets on SPUU with odd diamines are larger than those on SPUU with even diamines. This result indicates that the number of deformed platelets decreased with an increase in the degree of microphase separation. Since the surface concentration of soft segment (O/N) slightly depends on diamine structure, the blood compatibility assessed by the platelet adhesion and deformation of SPUU with various diamine components would be mainly governed by the nature of the polyether and the degree of phase mixing of hard and soft segments on its surface.

ACKNOWLEDGEMENTS

The authors wish to express their sincere thanks to Dr S. Inaba of Department of Blood Transfusion, Kyushu University Hospital. We thank Mr N. Sakamoto and Prof. Y. Yamamoto of Department of Mechanical Engineering, Faculty of Engineering, Kyushu University, for their generous advice, and assistance with XPS measurements.

REFERENCES

1 Bonart, R. and Muller, E. H. *J. Macromol. Sci.-Phys.* 1974, **B10**, 177, 345
2 Wilkes, G. L. and Abouzahr, S. *Macromolecules* 1981, **14**, 458
3 Kimura, I., Ishihara, H., Ono, H., Yoshikawa, H., Kawai, H. and Nomura, S. *Macromolecules* 1975, **7**, 355
4 Takahara, A., Tashita, J., Kajiyama, T. and Takayanagi, M. *Kobunshi Ronbunshu* 1982, **39**, 202
5 Takahara, A., Tashita, J., Kajiyama, T. and Takayanagi, M. *Rept. Progr. Polym. Phys. Jpn.* 1982, **25**, 841
6 Takahara, A., Tashita, J., Kajiyama, T. and Takayanagi, M. and MacKnight, W. J. *Polymer* 1985, **26**, 987
7 Takahara, A., Tashita, J., Kajiyama, T. and Takayanagi, M. 'International Progress in Urethanes', Vol. 4, (Eds. K. Ashida and K. C. Frisch), Technomic Publishers, 1985
8 Bonart, R., Morbitzer, L. and Rinke, H. *Kolloid-Z. Z. Polym.* 1970, **240**, 807
9 Lyman, D. J., Rev. *Macromol. Chem.* 1966, **1**, 191
10 Peebles, Jr., L. H. *Macromolecules* 1974, **7**, 873
11 Peebles, Jr., L. H. *Macromolecules* 1976, **9**, 59
12 Huh, D. S. and Cooper, S. L. *Polym. Eng. Sci.* 1971, **11**, 369
13 Nakayama, K., Ino, T. and Matsubara, I. *J. Macromol. Sci.-Chem.* 1969, **A3**, 1005
14 Ishihara, H., Kimura, I., Saito, K. and Ono, H. *J. Macromol. Sci.-Phys.* 1974, **B10**, 591
15 Hummel, D. O., Ellinghorst, G., Khatchatryan, A. and Stenzenberger, H. D. *Makromol. Chem.* 1979, **52**, 129
16 Williams, D. E. and Davis, L. E. 'Characterization of Metal and Polymer Surfaces', Vol. 2, Polymer Surfaces, (Ed. L. H. Lee), Academic Press, New York, 1977
17 Takahara, A., Kajiyama, T. and Takayanagi, M. *Rept. Progr. Polym. Phys. Jpn.* 1983, **26**, in press
18 Yonaha, C., Idezuki, Y., Hamaguchi, M., Watanabe, H., Mori, Y., Nagaoka, S., Kikuchi, T. and Tanzawa, H. *Jpn. J. Artif. Organs*, 1980, **9**, 228